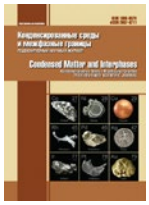

ISSN 1606-867X (Print)
ISSN 2687-0711 (Online)
Condensed Matter and Interphases
Kondensirovannye Sredy i Mezhfaznye Granitsy
https://journals.vsu.ru/kcmf/

Original articles

Research article
https://doi.org/10.17308/kcmf.2021.23/3678

Hydrothermal assisted conventional sol-gel method for synthesis of bioactive glass 70S30C

Ta Anh Tuan[1], Elena V. Guseva[1], Nguyen Anh Tien[2], Ha Tuan Anh[3], Bui Xuan Vuong[4], Le Hong Phuc[5]✉, Nguyen Quan Hien[5], Bui Thi Hoa[6,7], Nguyen Viet Long[8]

[1]Faculty of Chemical Technologies, Kazan National Research Technological University, 68 ul. K. Marksa, Kazan 420015, Tatarstan, Russian Federation

[2]Faculty of Chemistry, Ho Chi Minh City University of Education, 280 An Dương Vương str., Ward 4, District 5, Ho Chi Minh City, Vietnam

[3]Thu Dau Mot University, 6 Tran Van On str., Phu Hoa Ward, Thu Dau Mot City, Binh Duong Province 820000, Viet Nam

[4]Faculty of Pedagogy in Natural Sciences, Sai Gon University, Ho Chi Minh City, Vietnam

[5]Institute of Applied Mechanics and Informatics, 291 Dien Bien Phu str., District 03, Ho Chi Minh City 700000, Vietnam

[6]Institute of Theoretical and Applied Research, Duy Tan University, Hanoi 100000, Vietnam

[7]Faculty of Natural Sciences, Duy Tan University, Da Nang 550000, Vietnam

[8]Department of Electronics and Telecommunication, Sai Gon University, Ho Chi Minh City 700000, Vietnam

Abstract

Bioactive glasses (Bioglasses) are widely synthesized by the conventional sol-gel method consisting of two main steps for sol and gel formation. However, the conversion from sol to gel requires a long time (5–7 days). In this study, the hydrothermal system was used to quickly synthesize the bioactive glass by reducing the conversion time from sol to gel. The hydrothermal assisted conventional sol-gel method was applied for synthesis of the bioactive glass $70SiO_2$–30CaO (mol%) (noted as 70S30C). The synthetic glass was investigated by the physical-chemical techniques. The *"in vitro"* experiments in SBF (Simulated Body Fluid) solution was also performed to evaluate the bioactivity of synthetic material. The obtained results show that the bioactive glass 70S30C was successfully elaborated by using the hydrothermal assisted conventional sol-gel method. The consuming time was reduced compared to the conventional method. The physical-chemical characterization confirmed that the synthetic glass is amorphous material with mesoporous structure consisting of interconnected particles. The specific surface area, pore volume and average pore diameter of synthetic glass were 142.8 m^2/g, 0.52 cm^3/g, and 19.1 nm, respectively. Furthermore, synthetic bioactive glass exhibited interesting bioactivity when immersed in simulated body fluid (SBF) solution for 1 days and good biocompatibility when cultured in cellular media.

Keywords: Bioactive glass, Hydrothermal assisted sol-gel, Bioactivity, in vitro, Cell viability

For citation: Tuan T. A., Guseva E. V., Tien N. A., Anh H. T., Vuong B. X., Phuc L. H., Hien N. Q., Hoa B. T., Long N. V. Hydrothermal assisted conventional sol-gel method for synthesis of bioactive glass 70S30C. *Kondensirovannye sredy i mezhfaznye granitsy = Condensed Matter and Interphases*. 2021;23(4): 578–584. https://doi.org/10.17308/kcmf.2021.23/3678

Для цитирования: Туан Т. А., Гусева Е. В., Нгуен А. Т., Ань Х. Т., Выонг Б. С., Фук Л. Х., Хиен Н. К., Хоа Б. Т., Лонг Н. В. Стандартный метод золь-гель синтеза биоактивного стекла 70S30C с использованием гидротермальной системы. *Конденсированные среды и межфазные границы*. 2021;23(4): 578–584. https://doi.org/10.17308/kcmf.2021.23/3678

✉ Le Hong Phuc, e-mail: lhphuc76@yahoo.com

1. Introduction

In the past fifty years, bioactive glasses (bioglasses) have been developed and applied as artificial bone materials used as components in dental filling, implants, and bone grafting in orthopedic surgery to restore and repair damaged and diseased bones [1–2]. Their bioactivity is shown by the formation of a new layer of hydroxyapatite $Ca_{10}(PO_4)_6(OH)_2$ (HA) on the surfaces when they are implanted in defective and broken bone positions in the human body. The HA mineral is the inorganic component of human bone, so it is an interconnected linkage connecting the artificial graft made from bioglass and natural bone, through which the missing and broken bones are repaired and filled [3–5].

The first bioglass with the composition of $45SiO_2–24.5CaO–24.5Na_2O–6P_2O_5$ (wt%) (Denoted as 45S5) was discovered in 1969 by Larry Hench [6]. After this invention, many bioglass systems with different components such as 46S6, 58S, 55S, 70S30C, S53P4, etc. were studied, synthesized, and applied [1–2].

There are two main methods for bioglass synthesis. The first one is melting of precursors at high temperatures (melting method). The method can quickly prepare glass systems in large quantities. However, it requires synthesis processes at high temperatures (above 1350 °C) where volatile components such as P_2O_5 can be escaped, resulting in deviations in the composition of synthetic bioglasses; obtained materials often have low values of specific surface area [7]. The second one is to synthesize glass systems in solution undergoing sol- and gel-forming processes (sol-gel method). This process overcomes the disadvantages of melting method because it is performed at lower temperatures; resulting glass systems with larger values of specific surface area, leading to higher activity [8–9]. However, the sol-gel method requires long times for synthesis because the conversion from sol to gel usually takes from a few days to one week. Therefore, the modified sol-gel processes to shorten the synthesis times will be effective for the preparation of bioglass materials. On the other hand, variable synthesis processes can bring new properties of synthetic glass systems.

The purpose of this work is to synthesize the bioglass $70SiO_2–30CaO$ (mol%) by using the hydrothermal assisted sol-gel method, in which the synthesis time was greatly shortened. The physic-chemical characterizations and bioactivity of synthetic bioglass were investigated.

2. Experimental

2.1. Synthesis of bioactive glass

The bioglass $70SiO_2–30CaO$ (mol%) selected in this study is well-known and reported in the previous studies, in which it was synthesized by the sol-gel method [7–10]. The main precursors for the synthesis of bioglass included tetraethyl orthosilicate $Si(OCH_2CH_3)_4$ (TEOS, ⩾ 99.0%, Sigma-Aldrich), calcium nitrate tetrahydrate $Ca(NO_3)_2.4H_2O$ (CNT, ⩾ 98%, Merck). Hydrothermal assisted sol-gel method for bioglass synthesis is described as below. Firstly, 29.2 g of TEOS and 14.2 g of CNT were added in 25.2 g of distilled water. The molar ratio of H_2O/TEOS was selected as 10. The pH of mixture was adjusted to a value of 1.5 by adding 1M HNO_3 solution. The sol was formed after stirring for 1 hour at room temperature (32.2 °C). Next, the formed sol was put into a Teflon-lined stainless steel system, which was then heated in an oven at 150 C for 12 hours. After that, the resulting gel dried at 150 °C for 24 hours. Finally, the bioglass was obtained by sintering dried gel at 700 °C for 3 hours. To examine the phase evolution, the other samples of dried gel were heated at 800 and 1000 °C at the same times as above. The hydrothermal assisted sol-gel synthesis is briefly described in Fig. 1. It is worthy to mention that the consuming time of bioglass synthesis in this study was significantly shortened compared to the conventional sol-gel process [7, 10].

2.2. ''In vitro'' test in SBF solution

The bioactivity of synthetic bioglass was investigated by ''in vitro'' experiment according to Kokubo's method [11]. The glass material is immersed in simulate body fluid (SBF) solution at a stirring rate of 100 rpm and a temperature of 37 °C for 1, 2, 7, 10, and 15 days. The simulated body fluid (SBF) solution with inorganic ionic components similar to human blood, is synthesized in laboratory. The composition of simulated body fluid (SBF) solution is presented in the Table 1. After immersion in simulated body fluid (SBF) solution, the hydroxyapatite (HA) layer

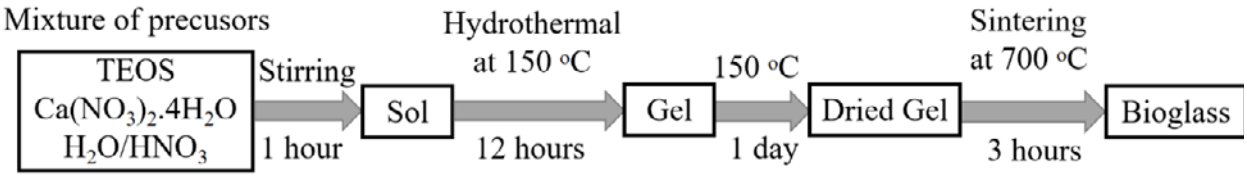

Fig. 1. Flow chart of hydrothermal assisted sol-gel synthesis of bioglass 70S

Table 1. Ionic concentration of SBF solution (mmol/L)

Composition	Na^+	K^+	Ca^{2+}	Mg^{2+}	Cl^-	HCO_3^-	HPO_4^{2-}
SBF	142.0	5.0	2.5	1.5	148.0	4.2	1.0
Plasma	142.0	5.0	2.5	1.5	103.0	27.0	1.0

will form on the surface of glass material if it is biologically active.

2.3. "In vitro" in cellular medium

"In vitro" tests were performed in according with the protocols reported by T. Mosmann [12]. The used culture environment was standard medium DMEM (Sigma Chemical Co., St. Louis, MO) consisting of 15 mM HEPES, 2 mM L-glutamine, 10% FBS (Fetal Bovine Serum), 100 UI/mL penicillin and 100 µg/mL streptomycin. Osteoblast-like $SaOS_2$ and endothelial-like Eahy926 were cultivated in DMEM at 37 °C in a humidified incubator with 5% CO_2 and 95% humidity.

The cytotoxicity was determined by using the colorimetric MTT assay [13]. The MTT (3-(4,5-Dimethylthiazol-2-yl)-2,5-diphenyl-tetrazolium bromide, a yellow tetrazole) is reduced to purple formazan in the mitochondria of living cells. The absorbance of this colored solution can be quantified by measuring at a certain wavelength (usually between 500 and 600 nm) by a spectrophotometer. The absorption maximum is dependent on the solvent employed. This reduction takes place only when mitochondrial reductase enzymes are active, and therefore conversion can be directly related to the number of living cells.

2.4. Physico-chemical characterization

The thermal properties of as-sintering bioglass were investigated by a Thermogravimetry-Differential Scanning Calorimetry (TG-DSC, SETERAM, LABSYS Evo). Powder sample was placed in a platinum crucible and then heated from room temperature to 1000 °C at a ratio of 10 $K.min^{-1}$ in dried air. From this analysis, the suitable temperature for the stabilization of synthetic bioglass was chosen. The specific surface area, pore size, and pore volume of synthetic bioglass were measured by N_2 adsorption/desorption using a micromeritics porosimeter (Quantachrome Instruments). The specific surface area was calculated using the Brunauer-Emmett-Teller (BET) method. The pore size and pore volume were derived from the desorption branch of the isotherm curve using the Barrett-Joyner-Halanda (BJH) technique. The morphology of the synthetic glass was observed by a Field Emission Scanning Electron Microscopy (FE-SEM, S-4800, Japan). The phase composition of the synthetic samples was investigated using X-ray powder diffraction (XRD, D8-Advance) with Cu-K_α radiation (λ = 1.5406Å). The samples were scanned in the range from 5 to 80° (2θ) with a step of 0.02°. The composition of synthetic glass was determined by X-ray fluorescence technique (PHILIPS, PW2400). The pH and Si, Ca, P concentration behaviors versus immersion times were determined by using the pH meter and inductively coupled plasma optical emission spectrometry (ICP-OES) (ICP 2060) method.

3. Results and discussion

3.1. Characterization of synthetic bioactive glass

TG-DSC curves of dried gel are represented in Fig. 2. Two mass-loss intervals were identified in the ranges of 30 – 279 °C and 279–658 °C. The first mass-loss with an endothermic peak at 155.6 °C, which is attributed to the removal of water [14].

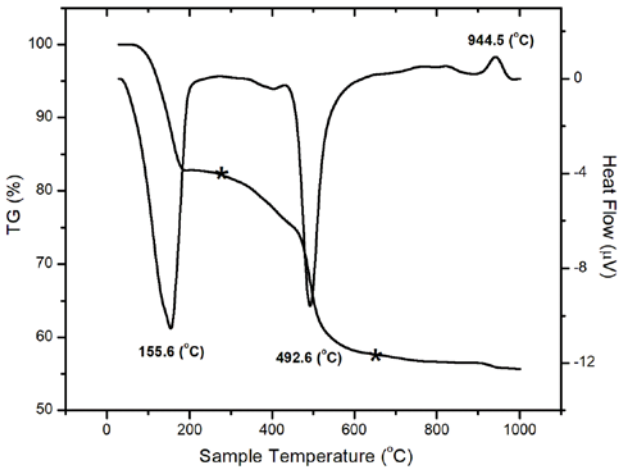

Fig. 2. TG-DSC analysis of as-sintering bioactive glass

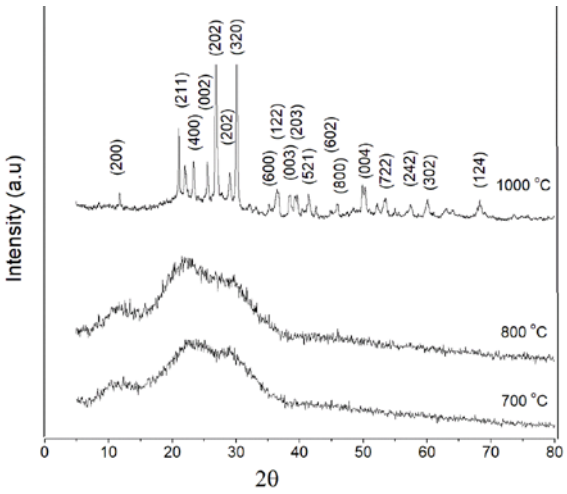

Fig. 3. XRD diagrams of sample heated at 700, 800 and 1000 °C

The second one with an endothermic peak at 492.6 °C is characteristic of the decomposition of NO_3^- groups [10]. An exothermic peak without the mass loss at 944.5 °C is related to the crystallization of $CaSiO_3$ phase [10, 14]. From the thermal analysis, the suitable temperature for calcination was identified 700 °C, where nitrates groups are completely removed.

Fig. 3 represents the XRD patterns of sample heated at 700, 800 and 1000 °C. The XRD diagram of synthetic bioactive glass obtained at 700 °C showed some broad diffraction halos, characteristic of the amorphous material. Thus, the bioactive glass $70SiO_2$–30CaO prepared by hydrothermal assisted sol-gel method still keeps the nature of glass like it was synthesized by the conventional sol-gel method [10, 14]. The composition of synthetic bioglass was analyzed using X-ray fluorescent spectroscopy (XRF). Compared to the calculated composition, the synthetic bioglas represents a moderate difference in composition (Table 2). This difference is explained by the amorphous structure of the synthetic bioglass, which leads to the uneven distribution of Ca, P, and O elements in the network of synthetic bioglass. The XRD diagram of sample heated at 1000 °C confirmed the crystallization of $CaSiO_3$ phase according to the TG-DSC analysis.

Table 2. The composition of bioglass $70SiO_2$–30CaO

Constituent (mol %)	SiO_2	CaO
Nominal	70	30
Analyzed	73.6	26.4

Textural and morphology of synthetic bioglass were investigated by N_2 adsorption/desorption and FE-SEM analyses (Fig. 4). The isotherm of synthetic bioglass shows type IV according to IUPAC nomenclature, typical of mesoporous material with the pore diameter in the range of 2–50 nm (Fig. 4a) [15–17]. The hysteresis loop is type H_2, given by complex pore structure in which network effect is important. The steep desorption branch can be attributed to pore-blocking or percolation in a narrow range of pore necks [16]. From the adsorption branch of isotherm curve, the pore size distribution and pore volume for synthetic bioglass were obtained by using the BJH model. The textural properties of synthetic bioglass are summarized in the table 3. The textural values of bioglass synthesized by the green synthesis are quite similar to those achieved for the bioglass with the same composition prepared by the conventional sol-gel method [10]. The morphology examination of synthetic bioglass was investigated by FE-SEM analysis. The observation shows obvious aggregations consisting of small particles, which were interconnected to form the mesoporous structure of the synthetic bioglass (Fig. 4b). According to the references, the Ca^{2+} immobilization onto the surface of silica particles modifies their surface chemistry, resulting in particle aggregation [18-19]. Under the effect of hydrothermal reaction, the Ca^{2+} ions could diffuse and act as strong cross-linkers between the silica particles, leading to highly aggregated particles.

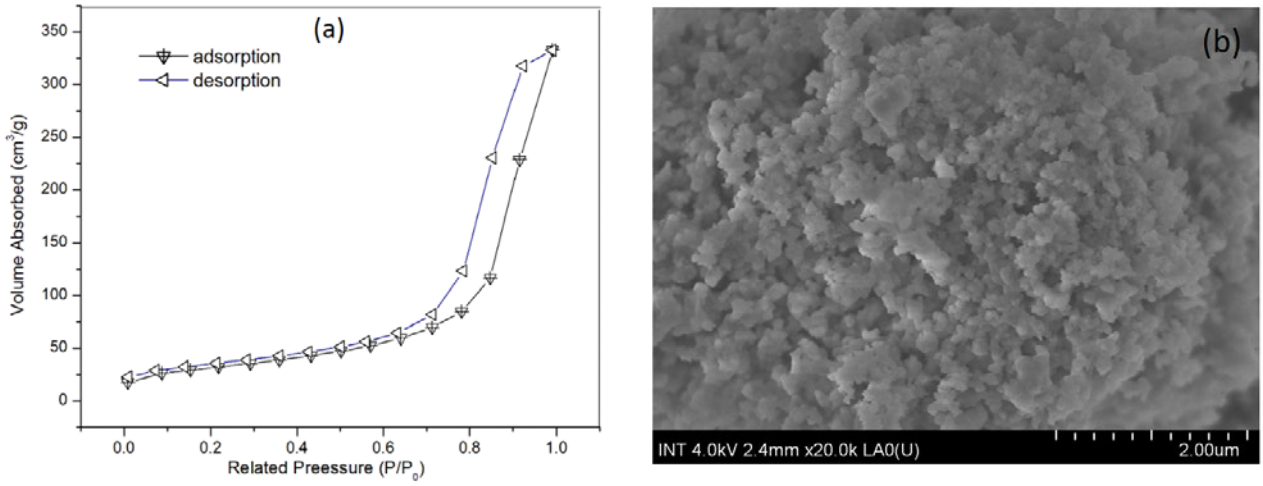

Fig. 4. a) N_2 adsorption/desorption isotherm and b) FE-SEM image of synthetic bioactive glass

Table 3. Nitrogen adsorption/desorption characterization of bioactive glass $70SiO_2$–30CaO

Sample	Specific Surface Area (m^2/g)	Total Pore Volume (cm^3/g)	Average Pore Diameter (nm)
$70SiO_2$–30CaO	142.8	0.52	19.1

3.2. Bio-mineralization

Fig. 5 represents the XRD diffractograms of synthetic bioactive glass after immersion in simulated body fluid (SBF) solution for 1, 2 and 7 days. The apatite mineral was confirmed by the well-defined appearance of two hydroxyapatite (HA) peaks at about 26° (002) and 32° (211) (JCPDS: 09432). This obtained result is similar to previous research for the same bioactive glass synthesized by the conventional sol-gel method and highlights the bioactivity of bioactive glass prepared by the hydrothermal assisted sol-gel method in this study [10, 14].

Fig. 6 shows the FE-SEM images of bioactive glass after different days in SBF. The formation of new HA was identified by a new crystalline layer, covering on the surfaces of glass samples after immersion in comparison with the sample before immersion presented in Fig. 4b.

3.3. Degradation of bioactive glass in SBF

The ionic behaviors in simulated body fluid (SBF) solution as a function of immersion time were represented in Fig. 7. The ionic changes are related to the surface reactions between the bioactive glass and the SBF solution [6, 20].

A significant increase of pH value was observed during the first seven days of immersion. This observation corresponds to the quick ion exchange of Ca^{2+} out of the bioactive glass and H^+ in the SBF solution as the following reaction:

$$(–Si–O–Si–O–)Ca^{2+} + H^+ \rightarrow$$
$$\rightarrow –Si–O–Si–OH + Ca^{2+} \quad (1)$$

The H^+ consumption in reaction 1 lead to an increasing pH value. After that, the pH value was almost constant due to the end of reaction 1.

The release of Si element is due to the dissolution of glass network in SBF solution by

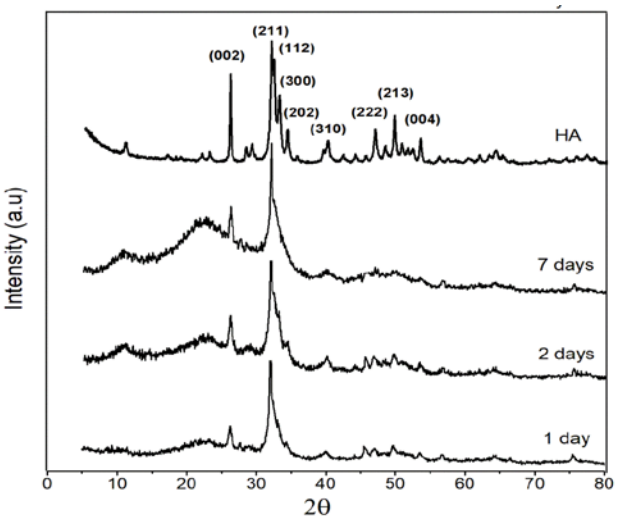

Fig. 5. XRD diagram of bioactive glass after immersion in SBF for 1, 2 and 7 days

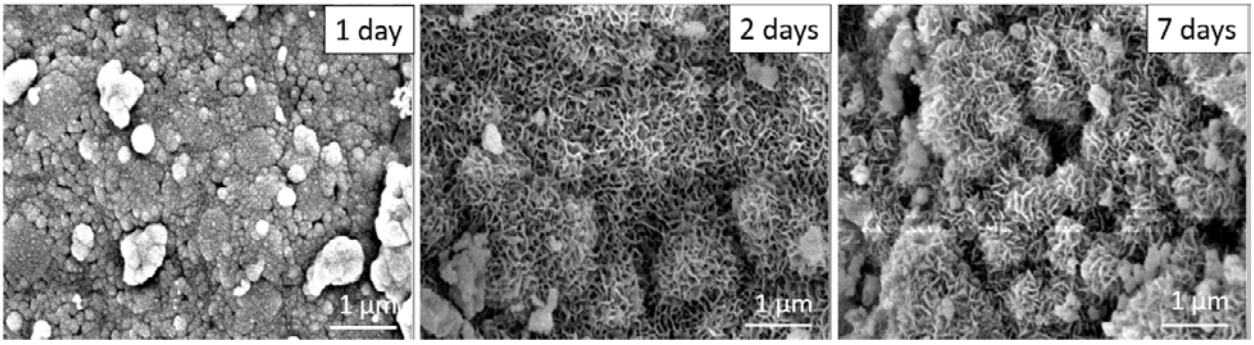

Fig. 6. FE-SEM images of bioactive glass after immersion in SBF for 1, 2 and 7 days

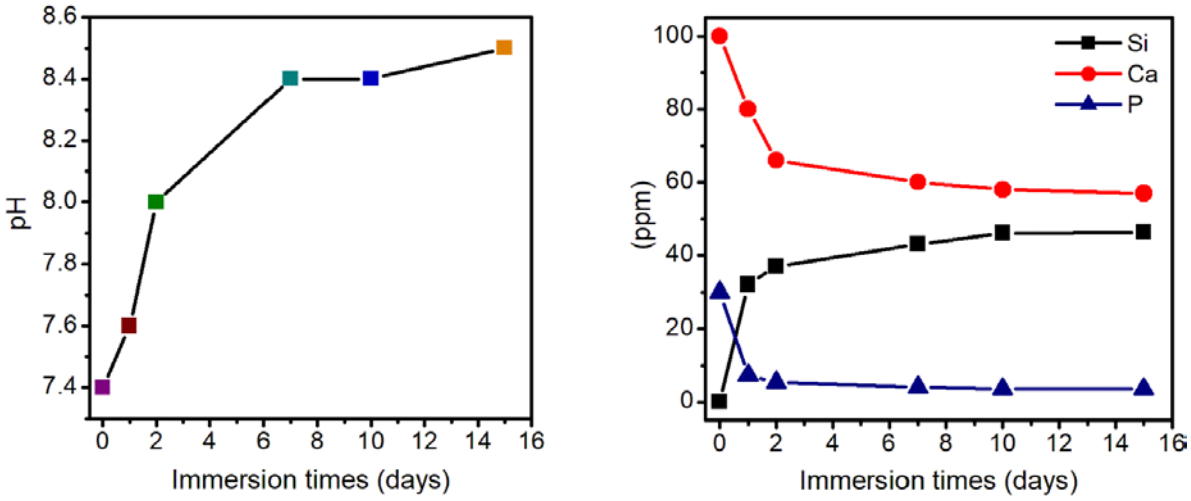

Fig. 7. Ionic concentrations of the SBF solution during ''in vitro'' experiment

breaking covalent bonds –Si–O–Si–OH following the reaction 2:

$$(–Si–O–Si–OH) + H_2O \rightarrow Si(OH)_4 \quad (2)$$

The Si concentration increased strongly during seven days of immersion, followed by the saturation in which the re-polymerization of silicic acid $Si(OH)_4$ occurs to form SiO_2 silica layer on the surface of the glass sample.

The presence of Ca and P in simulated body fluid (SBF) solution related to two sources. The first one was the Ca, P components available in initial solution. The second one was the Ca, P amounts released by the reaction of glass with SBF solution. Following the reaction 1, the Ca concentration in the SBF solution increases. However, a significant decrease in Ca component was identified during the whole immersion time. A similar observation was also identified for P amount. The decrease in Ca and P components was related to their consumption to precipitate the apatite layer on glass surface. The obvious consumption of Ca and P for the first two days of immersion in SBF confirmed the high bioactivity of synthetic bioactive glass. After 2 days of immersion, the Ca, P concentrations were almost stable while the pH value increased until 7 days. This phenomenon can be explained by the continuous degradation of bio-glass under reaction 1, simultaneously with the association of Ca and P components to form the HA layer on the surface of glass sample. The obtained result is consistent with the above analysis by the XRD, in which the HA layer was formed after 1 and 2 days of immersion.

3.4. Cell viability

The cell viabilities in the conditioned media of bioactive glass $70SiO_2–30CaO$ are represented in Fig. 8. After 2 days of culture, the cell viabilities

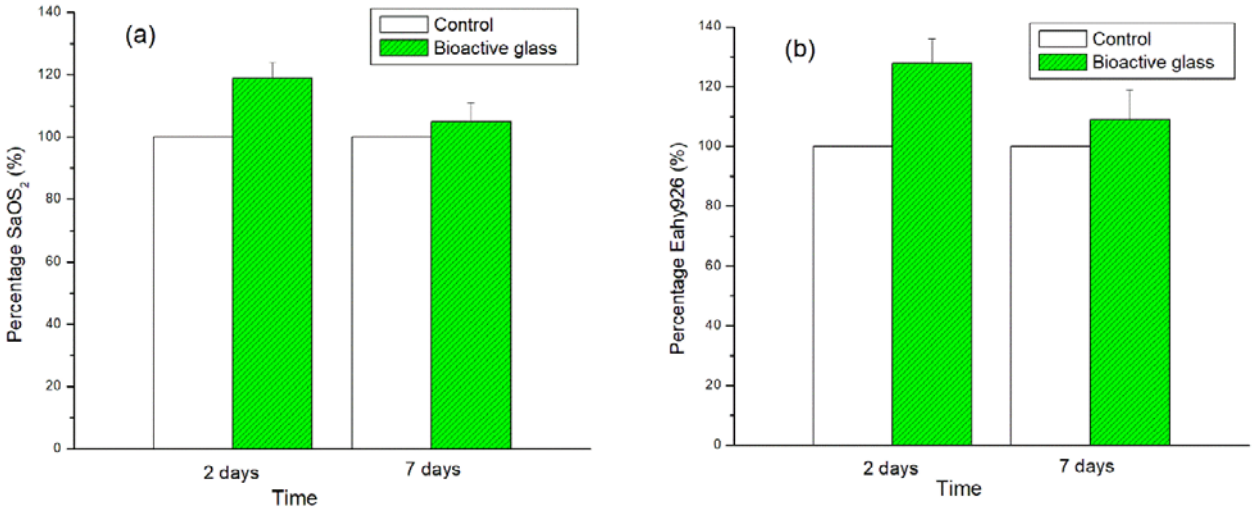

Fig. 8. Cell culturing viabilities on the bioactive glass after 2 and 7 days: (a) for osteoblast-like $SaOS_2$ and (b) for endothelial-like Eahy926

were 119 and 128% for osteoblast-like $SaOS_2$ and endothelial-like Eahy926, respectively. The viability of cells without contact with bioactive glass was fixed as control (100%). These obtained results confirmed the biocompatibility of synthetic bioactive glass with these two culturing cells. After 7 days, a decrease of Osteoblast-like $SaOS_2$ and endothelial-like Eahy926 viabilities was registered. That needs the renewal of culturing media. According to the standard ISO 10993-5 (Biological evaluation of medical devices – Part 5: Test for cytotoxicity, in vitro methods), the cell viability is expressed as a percentage relative to the control, set as 100% [21]. If the average cell viability of the tested samples is less than 70%, the material is cytotoxic. Following this standard, the bioactive glass $70SiO_2$-30CaO synthesized by hydrothermal assisted sol-gel method showed the absence of toxicity in comparison with the control sample. The synthetic bioactive glass in this study may find the potential applications as bone substitutes.

4. Conclusions

The bioactive glass $70SiO_2$–30CaO (mol%) was successfully prepared by hydrothermal assisted sol-gel method. The obtained glass is totally amorphous material and has a mesoporous structure. The in vitro assay in simulated body fluid (SBF) solution confirmed interesting bioactivity of synthetic glass by the formation of apatite phase after only one day of immersion in simulated body fluid (SBF) solution. The in vitro test in presence of cell culture confirmed good biocompatibility of synthetic bioactive glass. Especially, the synthetic processing is simple, short time-consuming in comparison with conventional sol-gel method.

Contribution of the authors

Ta Anh Tuan – Experiment, Analysis, Writing – original draft, Final conclusions. Elena V. Guseva – Investigation, Writing – review & editing. Nguyen Anh Tien – Investigation, Writing – review & editing. Ha Tuan Anh – Experiment, Investigation. Bui Xuan Vuong – Writing – review & editing. Le Hong Phuc – Experiment, Analysis. Nguyen Quan Hien – Experiment, Analysis. Bui Thi Hoa – Experiment, Analysis, Writing – review & editing. Nguyen Viet Long – Experiment, Analysis, Writing – original draft, Final conclusions.

Conflict of interests

The authors declare that they have no known competing financial interests or personal relationships that could have influenced the work reported in this paper.

References

1. Fernandez de Grado G., Keller L., Idoux-Gillet Y., Wagner Q., Musset A.-M., Benkirane-Jessel N.,Bone substitutes: a review of their characteristics, clinical use, and perspectives for large bone defects management, *Journal of Tissue Engineering*. 2018;9: 1–18. https://doi.org/10.1177/2041731418776819

2. Winker T., Sass F. A., Duda G. N., Schmidt-Bleek K. A review of biomaterials in bone defect healing, remaining shortcomings and future opportunities for bone tissue engineering. *Bone & Joint Research*. 2018;7(3): 232–243. https://doi.org/10.1302/2046-3758.73.BJR-2017-0270.R1

3. Oudadesse H., Dietrich E., Bui X. V., Gal Y. L., Pellen P., Cathelineau G. Enhancement of cells proliferation and control of bioactivity of strontium doped glass. *Applied Surface Science*. 2011;257(20): 8587–8593. https://doi.org/10.1016/j.apsusc.2011.05.022

4. Bui X. V., Dang T. H. Bioactive glass 58S prepared using an innovation sol-gel process. *Processing and Application of Ceramics*. 2019;13(1):98–103. https://doi.org/10.2298/PAC1901098B

5. Letaïef N., Lucas-Girot A., Oudadesse H., Meleard P., Pott T., Jelassi J., Dorbez-Sridi R. Effect of aging temperature on the structure, pore morphology and bioactivity of new sol-gel synthesized bioglass. *Journal of Non-Crystalline Solids*. 2014;402(15): 194–199. https://doi.org/10.1016/j.jnoncrysol.2014.06.005

6. Hench L. L., The story of bioglass. *Journal of Materials Science: Materials in Medicine*. 2006;17(11): 967–978. https://doi.org/10.1007/s10856-006-0432-z

7. Jones J. R. Review of bioactive glass: from Hench to hybrids. *Acta Biomaterialia*. 2013;9(1): 4457–4486. https://doi.org/10.1016/j.actbio.2012.08.023

8. Sepulveda S., Jones J. R., Hench L. L. Characterization of melt-derived 45S5 and sol-gel-derived 58S bioactive glasses. *Journal of Biomedical Materials Research*. 2001;58(6): 734–740. https://doi.org/10.1002/jbm.10026

9. Owens G. J., Singh R. K., Foroutan F., Alqaysi M., Han C. M., Mahapatra C., Kim H. W., Knowles J. C. Sol-gel based materials for biomedical applications. *Progress in Materials Science*. 2016;77: 1–79. https://doi.org/10.1016/j.pmatsci.2015.12.001

10. Martínez A., Izquierdo-Barba I., Vallet-Regí M. Bioactivity of a CaO-SiO_2 binary glasses system. *Chemistry of Materials*. 2000;12(10): 3080–3088. https://doi.org/10.1021/cm001107o

11. Kokubo T., Takadama H. How useful is SBF in predicting in vivo bone bioactivity. *Biomaterials*. 2006;27(15): 2907–2915. https://doi.org/10.1016/j.biomaterials.2006.01.017

12. Mosmann T. Rapid colorimetric assay for cellular growth and survival: application to proliferation and cytotoxicity assays. *Journal of Immunological Methods*. 1983;65: 55–63. https://doi.org/10.1016/0022-1759(83)90303-4

13. Tolosa L., Donato M. T., Lechón M. J. G. General cytotoxicity assessment by means of the MTT assay. *Methods in Molecular Biology*. 2015;1250: 333–348. https://doi.org/10.1007/978-1-4939-2074-7_26

14. Saravanapavan P., Hench L. L. Mesoporous calcium silicate glasses. I. Synthesis. *Journal of Non-Crystalline Solids*. 2003;318(1-2): 1–13. https://doi.org/10.1016/S0022-3093(02)01864-1

15. Valliant E. M., Turdean-Ionescu C. A., Hanna J. V., Smith M. E., Jones J. R. Role of pH and temperature on silica network formation and calcium incorporation into sol–gel derived bioactive glasses. *Journal of Materials Chemistry*. 2012;22: 1613–1619. https://doi.org/10.1039/C1JM13225C

16. Thommes M. Physical adsorption characterization of nanoporous materials. *Chemie Ingenieur Technik*. 2010;82(7): 1059–1073. https://doi.org/10.1002/cite.201000064

17. Thommes M., Kaneko K., Neimark A. V., Olivier J. P., Rodriguez-Reinoso F., Rouquerol J., Sing K. S. W. Physisorption of gases, with special reference to the evaluation of surface area and pore size distribution. *Pure and Applied Chemistry*. 2015;87(9,10): 1–19. https://doi.org/10.1515/pac-2014-1117

18. Zheng K., Boccaccini A. R. Sol-gel processing of bioactive glass nanoparticles: A review. *Advances in Colloid and Interface Science*. 2017;249: 363–373. https://doi.org/10.1016/j.cis.2017.03.008

19. Xavier K., Charlotte V., Jean-Marie N. Deeper insights into a bioactive glass nanoparticle synthesis protocol to control its morphology, dispersibility, and composition. *ACS. Omega*. 2019;4(3): 5768–5775. https://doi.org/10.1021/acsomega.8b03598

20. Galarraga-Vinueza M. E., Mesquita-Guimaraes J., Magini R. S., Souza J. C. M., Fredel M. C., Boccaccini, A. R. Mesoporous bioactive glass embedding propolis and cranberry antibiofilm compounds. *Journal of Biomedical Materials Research Part A*. 2018;106(6): 1614–1625. https://doi.org/10.1002/jbm.a.36352

21. Standard ISO 10993-5, Biological evaluation of medical devices Part 5: Test for in vitro cytotoxicity. 2009.

Information about the authors

Ta Anh Tuan, PhD student, Faculty of Chemical Technologies, Kazan National Research Technological University, Kazan, Tatarstan, Russian Federation; email: taanhtuan84pt@hpu2.edu.vn. ORCID iD: https://orcid.org/0000-0002-7254-1637.

Elena V. Guseva, PhD in Chemistry, Associate Professor, Faculty of Chemical Technologies, Kazan National Research Technological University, Kazan, Tatarstan, Russian Federation; email: leylaha@mail.ru. ORCID iD: https://orcid.org/0000-0002-2367-8012.

Nguyen Anh Tien, PhD in Chemistry, Associate Professor, Chief of General and Inorganic Chemistry Department, Ho Chi Minh City University of Education, Vietnam; e-mail: tienna@hcmue.edu.vn. ORCID iD: http://orcid.org/0000-0002-4396-0349.

Ha Tuan Anh, Thu Dau Mot University, Thu Dau Mot City, Vietnam; e-mail: anhht@tdmu.edu.vn. ORCID iD: https://orcid.org/0000-0002-1067-0863.

Bui Xuan Vuong, Associate Professor, Faculty of Natural Sciences, Sai Gon University, Ho Chi Minh City, Vietnam; e-mail: bxvuong@sgu.edu.vn. ORCID iD: https://orcid.org/0000-0002-3757-1099.

Le Hong Phuc, Institute of Applied Mechanics and Informatics, Ho Chi Minh City, Vietnam; e-mail: lhphuc@hcmip.vast.vn. ORCID iD: https://orcid.org/0000-0003-2353-7495.

Nguyen Quan Hien, Ho Chi Minh City Institute of Physics, Vietnam Academy of Science and Technology, Ho Chi Minh City, Vietnam; e-mail: quanhiengv@yahoo.com.vn. ORCID iD: https://orcid.org/0000-0002-5814-6745.

Bui Thi Hoa, Institute of Theoretical and Applied Research, Duy Tan University, Hanoi, Vietnam; Faculty of Natural Sciences, Duy Tan University, Da Nang, Vietnam; e-mail: buithihoa2@duytan.edu.vn. ORCID iD: https://orcid.org/0000-0003-0274-3716.

Nguyen Viet Long, Department of Electronics and Telecommunication, Sai Gon University, Ho Chi Minh City, Vietnam; e-mail: nguyenviet_long@yahoo.com. ORCID iD: https://orcid.org/0000-0003-0129-9879.

Received April 20, 2021; approved after reviewing May 27, 2021; accepted for publication September 15, 2021; published online December 25, 2021.